The formation of rhodochrosite–smithsonite ($MnCO_3$–$ZnCO_3$) solid-solutions at 5°C

MICHAEL E. BÖTTCHER*

Geochemical Institute, Georg-August-University, Goldschmidtstr.1, D-37077 Göttingen, Germany

Abstract

$Mn_XZn_{(1-X)}CO_3$ solid-solutions were prepared at 5°C by precipitation from metal-bearing bicarbonate solutions. The solids were identified by X-ray powder diffraction and infrared spectroscopy. Zn^{2+} ions substitute extensively for Mn^{2+} ions in the crystal lattice of anhydrous rhombohedral carbonates. Throughout the 24 h during which the experiments were conducted, the aqueous solutions remained undersaturated with respect to pure oxides, sulphates, hydroxides and hydroxysulphates. The solutions, however, were supersaturated with $Mn_XZn_{(1-X)}CO_3$ of any given composition. Besides the anhydrous rhombohedral carbonates, $Zn_4(OH)_2(CO_3)_3{\cdot}4H_2O$ was precipitated from an aqueous solution with initially high Zn^{2+} concentration. The negative logarithm of the solubility product of $Zn_4(OH)_2(CO_3)_3{\cdot}4H_2O$ was estimated theoretically to be 43.9 (25°C). Remaining saturation with respect to $Zn_4(OH)_2(CO_3)_3{\cdot}4H_2O$ was calculated accordingly. The suggestion is made that hydrated zinc hydroxycarbonate is metastable under the experimental conditions used here, but that it should transform into anhydrous carbonates.

KEYWORDS: rhodochrosite, smithsonite, solid-solutions, zinc hydroxycarbonate, synthesis.

Introduction

A nearly complete natural rhodochrosite–smithsonite ($MnCO_3$–$ZnCO_3$) solid-solution series has been found in the oxidized zone of the ore body at Broken Hill, N.S.W., Australia (Birch, 1986; Böttcher *et al.*, 1993; Böttcher *et al.*, in prep.). The series was studied by X-ray powder diffraction, electron microprobe, stable isotope techniques, infrared and Raman spectroscopy. Given their habit and their encrustation of concretionary goethite (α-FeOOH) and coronadite ($Pb_2Mn_8O_{16}$), a low-temperature formation of these carbonate phases was proposed and confirmed by oxygen isotope measurements (Böttcher *et al.*, 1993).

The formation of rhodochrosite–smithsonite solid-solutions may be important for supergene reactions in ore deposits and for the purification processes of industrial waters containing transition elements. Its quantitative significance has probably previously been underestimated. However, although Böttcher *et al.* (1993) applied a tentative thermodynamic model to estimate the metal-activity ratios of the aqueous solutions from which the Broken Hill carbonates were precipitated, less is known on the formation conditions of rhodochrosite–smithsonite solid-solutions. Apart from its pure end-members, the system $MnCO_3$–$ZnCO_3$–H_2O has not been hitherto investigated experimentally. In the study described here, preliminary experiments were conducted to synthesize rhodochrosite–smithsonite solid-solutions from aqueous solutions at 5°C.

* Present address: Institute of Chemistry and Biology of the Marine Environment (ICBM), Microbiogeochemistry, Carl von Ossietzky University, P.O. Box 2503, D-26111 Oldenburg, Germany

Methods

Rhodochrosite–smithsonite solid-solutions were synthesized by the addition of 100 ml of a 0.4 M $KHCO_3$ solution (presaturated at 22°C with CO_2 from a gas tank (99.995 %; Messer Griesheim)) to 100 ml of a 0.1 M $(Mn,Zn)SO_4$ solution at 5°C. The sulphate solutions were prepared under N_2 by the dissolution of reagent grade chemicals (Merck) in deionized water previously degassed with N_2.

Mineralogical Magazine, September 1995, Vol. 59, pp. 481–488

The precipitates were allowed to age undisturbed in contact with the mother liquid at 5 ± 1°C in closed Duran® glass bottles (500 cm^3) for about 24 h. At the end of each run, the pH of the solution was measured under air-tight conditions by an ion-selective combination micro-electrode (Ingold 10 402 3522 U402-M3-S7/60) and a digital pH-meter (Knick Portamess 645). The accuracy was ± 0.02 pH units. The electrode had been calibrated with buffers 4.00 and 6.88 (Riedel de Häen). Immediately after the pH measurements, the solids were separated from the solutions by membrane filtration using a Teflon®-coated N_2-pressure filtration-apparatus and polyacetate filters (0.45 μm porosity; Sartorius). Finally they were washed with methanol and dried at 60°C.

The mineral phases in the precipitates were identified by X-ray powder diffraction (Philips-XRD goniometer and Ni-filtered Cu-$K\alpha$ radiation) and infrared spectroscopy (683 Perkin Elmer spectrophotometer; KBr-pellet technique). The composition of the synthetic $Mn_xZn_{(1-x)}CO_3$ solid-solutions was estimated from the position of the $d(10\bar{1}4)$ peak in the X-ray diffractogram and the ν4 absorption band position in the infrared spectra. The $d(10\bar{1}4)$ spacing was assumed to bear a linear relationship with the chemical composition according to the following expression:

$$ZnCO_3\ (mol\%) = 1097.7 \cdot (2.839 - d(10\bar{1}4)(Å)) \quad (1)$$

The $d(10\bar{1}4)$ values of rhodochrosite and smithsonite were calculated from data given by Effenberger *et al.* (1981). Based on the results of Böttcher *et al.* (1993), a linear variation of the ν4 absorption maximum with increasing substitution of Mn^{2+} by Zn^{2+} was assumed to obey the following relationship:

$$ZnCO_3\ (mol\%) = 5.88 \cdot (\nu4(cm^{-1}) - 725.5) \quad (2)$$

The ν4 data for rhodochrosite and smithsonite were taken from Böttcher *et al.* (1992) and Böttcher *et al.* (1993), respectively. The estimated compositions are believed to be accurate to within ± 5 mol%.

After appropriate dilution and the addition of CsCl as an ionization buffer, the final aqueous solutions were analysed for Mn^{2+} and Zn^{2+} by atomic absorption spectrophotometry (Perkin Elmer 400) using an air-acetylene flame. K^+ and Mn^{2+} or Zn^{2+} AAS-standard solutions (Titrisol®, Merck) were added to the blanks and aqueous standards to match the matrix composition of the diluted run solutions. The accuracy of the analyses was estimated to be better than ± 5 %. The sum of the dissolved carbonate species (ΣC) and the partitioning of the individual species were calculated from the measured pH values and the cation concentrations, based on an

TABLE 1. Chemical compositions of aqueous solutions and final precipitates. X^*_{Mn}, X_{Mn}: mole fraction of the aqueous solution and $Mn_xZn_{(1-x)}CO_3$ solid-solution, respectively

	Run #1	#2	#3
Initial solution:			
pH	7.41	7.41	7.41
K^+ (mmol/l)	200	200	200
Mn^{2+} (mmol/l)	50.0	37.5	25.0
Zn^{2+} (mmol/l)	0	12.5	25.0
ΣC (mmol/l)	215	215	215
SO_4^{2-} (mmol/l)	50	50	50
X^*_{Mn}	1.00	0.75	0.50
Final solution:			
pH	6.78	6.81	6.79
Mn^{2+} (mmol/l)	5.6	4.5	3.3
Zn^{2+} (mmol/l)	0	1.5	2.7
ΣC (mmol/l)	154	152	153
X^*_{Mn}	1.00	0.75	0.55
Final precipitate:			
X_{Mn}	1.00	0.68 (±0.2)	0.51 (+0.1)*

*: Minor $Zn_4(OH)_2(CO_3)_3 \cdot 4H_2O$ was identified by XRD and IR.

electron balance approach described by Plummer and Busenberg (1982). The distribution and activities of the dissolved species were calculated with the Solmineq.88 PC/Shell computer program (Kharaka *et al.*, 1988; Wiwchar *et al.*, 1988) based on an ion-pair model described by Kharaka *et al.* (1988). The dissociation constants at 5°C of $MnHCO_3^+$ and $ZnHCO_3^+$ are from Lesht and Bauman (1978) and Ryan and Bauman (1978). For $ZnSO_4^0$ and the zinc hydroxy complexes they are from the Solmineq.88 database. The values for $MnOH^+$and $MnSO_4^0$ were calculated according to an isocoulombic approach (Böttcher and Usdowski, 1990). The equilibrium constants for the CO_2–H_2O system are from Plummer and Busenberg (1982).

Results and discussion

The experimental conditions and analytical results are compiled in Table 1.

Saturation calculations

A thermodynamic analysis of the initial run solutions indicated the presence of significant supersaturations with respect to pure rhodochrosite (runs #1–#3), and smithsonite, $Zn_4(OH)_2(CO_3)_3{\cdot}4H_2O$ (see below) and hydrozincite (runs #2 and 3). The solution however, was undersaturated with respect to pure oxides, sulphates, hydroxides and hydoxysulphates (Table 2). According to the calculated species distribution, 39% of the total dissolved zinc and 43% of the total dissolved manganese concentrations (Table 1) were initially present as Zn^{2+} and Mn^{2+}, respectively. From the Lippmann phase diagram in Fig.1 it can be seen that the initial aqueous solutions were also supersaturated with respect to $Mn_xZn_{(1-x)}CO_3$ solid-solutions of any given composition. The phase diagram was constructed according to Glynn and Reardon (1990), and represents the equilibrium conditions for the system $MnCO_3$–$ZnCO_3$–H_2O at 5°C, assuming ideal mixing behavior for the rhodochrosite–smithsonite solid-solutions.

As a result of the precipitation of carbonates and hydrous hydroxycarbonates, the solution's pH decreased (Table 1) and dissolved CO_2 was produced according to the overall reaction (written for $Mn_xZn_{(1-x)}CO_3$ solid-solutions)

$$x\mathrm{Mn}^{2+} + (1-x)\mathrm{Zn}^{2+} + 2\mathrm{HCO}_3^- \rightarrow \mathrm{Mn}_x\mathrm{Zn}_{(1-x)}\mathrm{CO}_3 + \mathrm{CO}_2 + \mathrm{H}_2\mathrm{O} \quad (3)$$

Therefore, following the initial mixing-step, supersaturation with respect to carbonate minerals was additionally caused by CO_2 escaping into the incompletely filled reaction vessels.

According to the speciation calculations on the final run solutions, 45% of the measured dissolved zinc and 48% of the total dissolved manganese existed as free Zn^{2+} and Mn^{2+}, respectively. The concentration of dissociated species is therefore slightly increased with respect to the initial solutions. This is due to the influence of decreasing pH and the total ion's concentrations on the partitioning of the dissolved species. At the end of the experiments and after a reaction time of 24 h, the aqueous solutions were still supersaturated with the anhydrous carbonates, but saturation (run #3) and even undersaturation (run #2) with hydrozincite and $Zn_4(OH)_2(CO_3)_3{\cdot}4H_2O$, was achieved for the Zn^{2+} bearing solutions (Table 2; Fig.1).

It should be noted that the solubility product of hydrozincite used in the present calculations was measured on synthetic material by Schindler *et al.* (1969). The results should be valid for the present experiments. Natural hydrozincite specimens were found experimentally to be less soluble than synthetic materials (Zachara *et al.*, 1989). These differences have been attributed to structural characteristics, the degree of hydration and/or solids stoichiometric

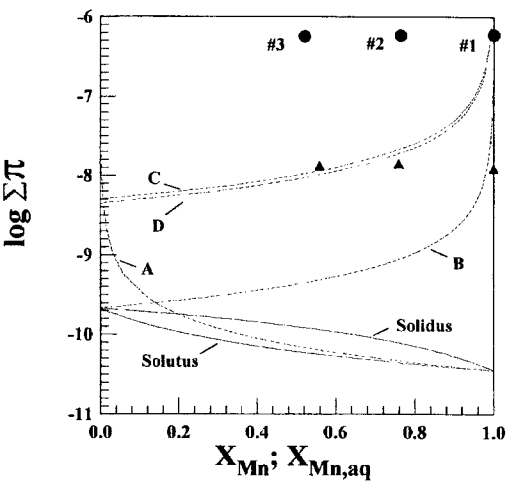

FIG. 1. Lippmann phase diagram for the System $ZnCO_3$–$MnCO_3$–H_2O (5°C, 1 bar total pressure). End-member pK-values are 9.67 (smithsonite) and 10.45 (rhodochrosite) (Table 2). $\Sigma\Pi = (\{Mn^{2+}\} + \{Zn^{2+}\}) \cdot \{CO_3^{2-}\}$; {}: activities. X_{Mn} and $X_{Mn,aq}$ are the solid-solutions manganese mole fraction and the aqueous solutions activity fraction, respectively. Respective equilibrium compositions of the $Mn_xZn_{(1-x)}CO_3$ solid-solutions and aqueous solutions are presented by the solidus and solutus curves (Böttcher *et al.*, 1993; Glynn and Reardon, 1990). $\Sigma\Pi$ values are also given at saturation with respect to pure $MnCO_3$ (A), $ZnCO_3$ (B), $Zn_4(OH)_2(CO_3)_3{\cdot}4H_2O$ (C; pH = 6.8) and hydrozincite (D; pH = 6.8). (●): initial solutions; (▲): final solutions.

TABLE 2. Calculated saturation indices (SI) for the initial and final run solutions with respect to selected solids. SI values < 1 and > 1 indicate, undersaturation and supersaturation, respectively

Solid phase	Initial/final SI			logK
	Run #1	Run #2	Run #3	
$MnCO_3$	4.2/2.5	4.1/2.5	3.9/2.3	−10.45
$Mn(OH)_2$	−5.1/−7.2	−5.3/−7.3	−5.4/−7.5	−11.72
$MnSO_4$	−7.8/−8.6	−7.9/−8.7	−8.1/−8.8	3.49
MnO	−6.6/−8.7	−6.7/−8.7	−6.9/−8.9	19.21
$ZnCO_3$	–	2.8/1.2	3.1/1.4	−9.67
ε-$Zn(OH)_2$	–	−1.0/−3.0	−0.7/−2.8	−16.47*
$ZnSO_4$	–	−9.4/−10.2	−9.1/−9.9	4.48
ZnO	–	−0.6/−2.6	−0.3/−2.4	12.54
$Zn(SO_4)_{0.5}OH$	–	−1.0/−2.4	−0.7/−2.1	−10.25*
$Zn(SO_4)_{0.25}(OH)_{1.5}$	–	−0.5/−2.2	−0.2/−1.9	−13.90*
$Zn(CO_3)_{0.4}(OH)_{1.2}$	–	1.6/−0.3	1.9/0	−14.87*
$Zn(CO_3)_{0.75}(OH)_{0.5}\cdot H_2O$	–	1.5/−0.3	1.8/0	−11.0"

Solubility products at 5°C (log K) are from Ball *et al.* (1987), Böttcher (1993), Johnson *et al.* (1992) and Kharaka *et al.* (1988) except for (*) which are 25°C values (Ball *et al.*, 1987; Mann and Deutscher, 1980; Schindler, 1967; Schindler *et al.*, 1969). ("): calculated from ΔG_f^o values as described in the text.

differences between natural and synthetic hydrozincites (Feitknecht and Oswald 1966; Jambor, 1964; Schindler *et al.*, 1969; Zachara *et al.*, 1989). Unfortunately, the solubility product of $Zn_4(OH)_2(CO_3)_3\cdot 4H_2O$ has not been hitherto determined. Therefore, the solubility product constant at 25°C was calculated from the standard Gibbs free energies of formation (ΔG_f^o) of the aqueous ions (Wagman *et al.*, 1982) and a hypothetical value for the solid which is estimated according to a method described by La Iglesia and Félix (1994). The thermodynamic properties of the basic polyhedral units of the hydrated zinc hydroxycarbonate were taken from La Iglesia and Félix (1994), except for $Zn(OH)_2$ (ΔG_f^o = −555.6 kJ/mol; Schindler, 1967). The application of the estimation procedure to $Zn_4(OH)_2(CO_3)_3\cdot 4H_2O$ yields ΔG_f^o = −3684.5 ± 5.1 kJ/mol. Based on one mole Zn^{2+} per formula ($Zn(OH)_{0.5}(CO_3)_{0.75}$ H_2O), the negative logarithm of the solubility product is calculated to be 11.0 ± 0.2 at 25°C (Table 2).

From a comparison with the temperature-dependent variation of the solubility products of artinite and hydromagnesite (Johnson *et al.*, 1992), the comparable data for the hydroxyl-bearing zinc minerals are expected to be similar. Therefore the saturation indices, calculated using the 25°C values in Table 2, are probably slightly too positive.

The precipitated solids

In accordance with the thermodynamic calculations, a fine-grained, pale pink precipitate was formed immediately due to the mixing of the $KHCO_3$ and $(ZnMn)SO_4$ solutions at 5°C. The intensity of the pinkish colour increased and the precipitation rates decreased with increasing Mn^{2+} concentrations of the initial solutions. The X-ray patterns and parts of the infrared spectra of the final precipitates are displayed in Figs. 2 and 3. They indicate that rhombohedral carbonates as the main solid phases formed. Pure $MnCO_3$ was the only precipitate in run #1. The reduction of the $d(10\bar{1}4)$ spacing, and the shift of the infrared absorption bands to higher values than for pure rhodochrosite indicate that Mn^{2+} in the rhodochrosite lattice is replaced by Zn^{2+} and that $Mn_xZn_{(1-x)}CO_3$ solid-solutions were formed in runs #2 and #3. The application of equations (1) and (2) to the #2 and #3 precipitates gives average manganese mole fractions (X_{Mn} = Mn/(Mn + Zn)) of 0.7 and 0.5 respectively. However, the X-ray peaks and also the infrared bands for the carbonate formed during run #2 are broadened with respect to the pure anhydrous solids and shoulders appear at the side towards an increased zinc concentration with respect to the average value. This indicates a solid-solution composition within an estimated range of about ± 0.2, where the Mn^{2+}-rich phase dominates and the Zn^{2+}-rich composition is only observed as the minor phase (Fig. 2 and 3). Although the ideal exchange equilibrium constant calculated according to Böttcher *et al.* (1993) (K_{eq} = 6) predicts a relative enrichment of Mn^{2+} with respect to Zn^{2+} in the solid, the Mn^{2+}/Zn^{2+} ratios of the main $Mn_xZn_{(1-x)}CO_3$ solids and the initial aqueous solutions are similar (Table 1). This case, where essentially no cationic

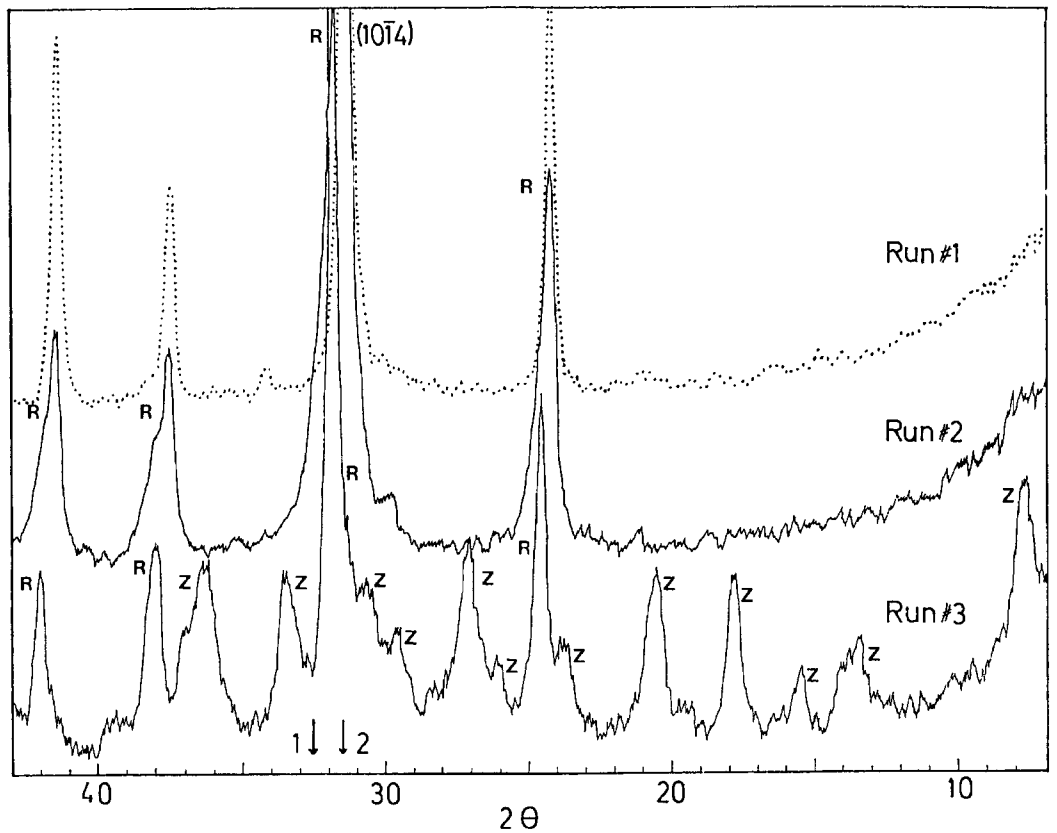

FIG. 2. X-ray patterns of the final precipitates. Pointed line: Pure $MnCO_3$ (run #1). R: $Mn_xZn_{(1-x)}CO_3$ solid-solutions; Z: $Zn_4(OH)_2(CO_3)_3{\cdot}4H_2O$ (with minor substitution of Zn^{2+} by Mn^{2+}). 1 and 2: positions of the (10$\bar{1}$4) peaks of pure $ZnCO_3$ and $MnCO_3$, respectively (Effenberger *et al.*, 1981).

fractionation appears between aqueous and solid-solution is due to the spontaneous precipitation from highly supersaturated solutions. Comparable results were observed previously for the systems $MnCO_3$–$CaCO_3$ and $CdCO_3$–$CaCO_3$, (Böttcher, 1993; Königsberger *et al.*, 1991). With decreasing rates of precipitation, cation fractionation during solid-solution formation should increase (Lorens, 1981). For trace concentrations under ideal conditions the fractionation will be limited by the equilibrium constant. Therefore, the observed compositional range of the solid-solutions is probably the result of decreasing precipitation rates during the reaction progress in experiments #2 and #3.

By comparing Figs. 2 and 3 with the published X-ray patterns and the infrared spectra of synthetic (hydrous) zinc hydroxycarbonates (Feitknecht and Oswald, 1966; Jambor, 1964), it appears that minor amounts of $Zn_4(OH)_2(CO_3)_3{\cdot}4H_2O$ were formed in run #3. Small shifts are observed for the *d*-spacings of the hydrous precipitate with respect to the patterns of the pure solid (Feitknecht and Oswald, 1966), probably due to crystallinity differences or to the substitution of Zn^{2+} by minor Mn^{2+} in the lattice of $Zn_4(OH)_2(CO_3)_3{\cdot}4H_2O$ formed in run #3. The observed compositions of the final precipitates are in fair agreement with the results of the thermodynamic analysis (Tables 1 and 2).

Precipitation order

The order in which the hydrated and anhydrous carbonates in run #3 were precipitated can not be deduced from the thermodynamic analysis alone, because the aqueous solutions remained supersaturated with respect to the relevant phases during the experiments (Table 2). Under Mn^{2+}-free but otherwise similar experimental conditions to run #3,

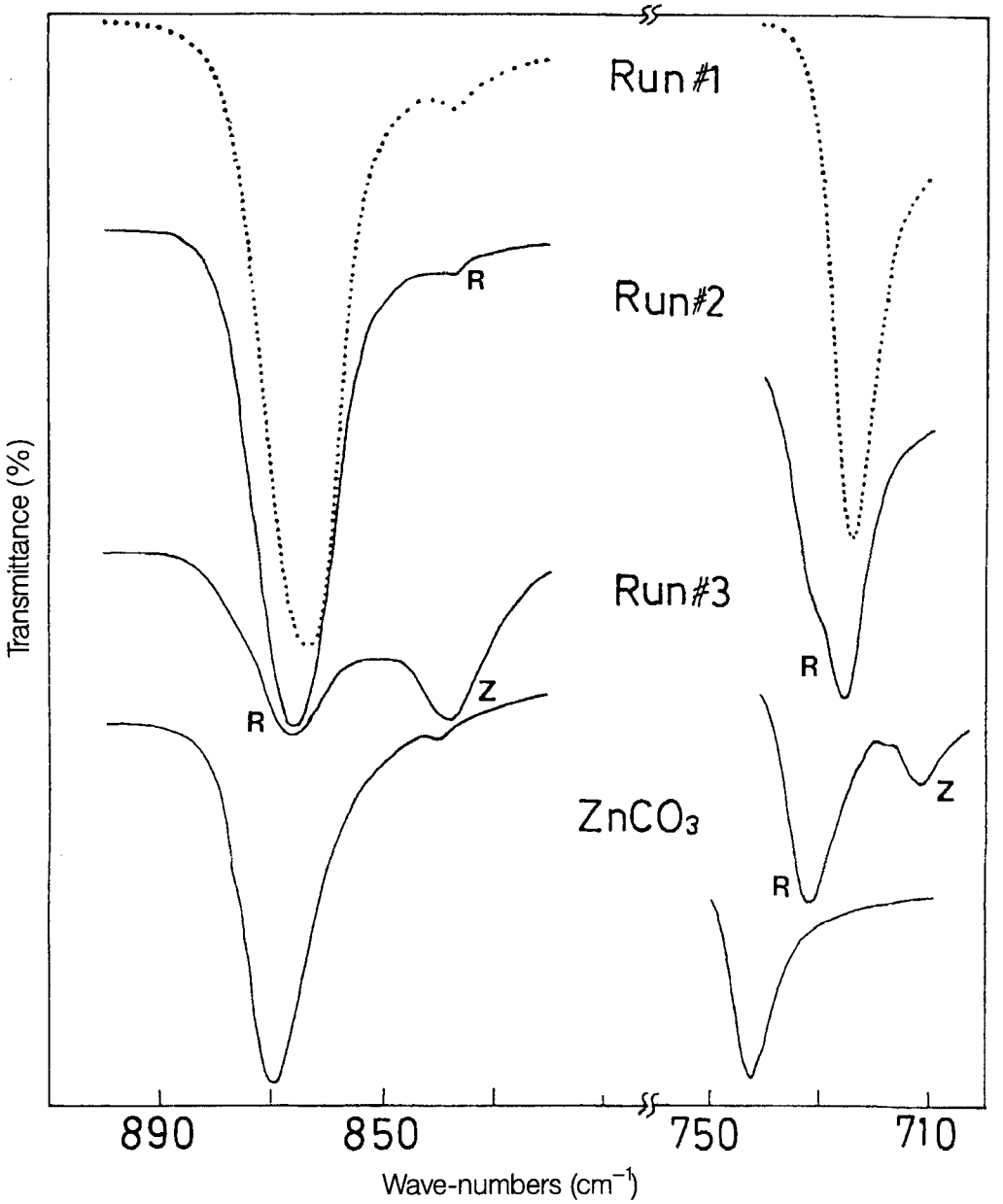

FIG. 3. Selected parts of the infrared spectra of the final precipitates. Pointed line: Pure $MnCO_3$ (run #1). R: $Mn_XZn_{(1-X)}CO_3$ solid-solutions; Z: $Zn_4(OH)_2(CO_3)_3{\cdot}4H_2O$; $ZnCO_3$: natural smithsonite from El Cobre (Mexico) ($Zn_{0.971}Ca_{0.024}Mg_{0.004}Mn_{0.001}CO_3$).

Kraut (1897) observed the initial formation of anhydrous $ZnCO_3$ which subsequently transformed to hydrated zinc carbonate or $Zn_5(OH)_6(CO_3)_2{\cdot}H_2O$, depending on the treatment. While a mixture of $Zn_4(OH)_2(CO_3)_3{\cdot}4H_2O$ and hydrozincite was synthesized by bubbling CO_2 into a suspension of $Zn_5(OH)_6(CO_3)_2{\cdot}H_2O$ (Feitknecht and Oswald, 1966; Jambor, 1964), pure $Zn_4(OH)_2(CO_3)_3{\cdot}4H_2O$

was the product of mixing zinc nitrate and sodium bicarbonate solutions (Feitknecht and Oswald, 1966); this altered to $ZnCO_3$ in contact with the mother solution. The formation of anhydrous smithsonite was observed during the interaction of zinc chloride solutions with calcite (Kaushansky and Yariv, 1986). It is obvious that the relation between the different hydrous and anhydrous Zn-bearing carbonates seems to be strongly controlled by reaction kinetics, the formation of metastable phases and depends on a number of (experimental) boundary conditions. However, from the calculated saturation indices for the rhombohedral carbonates and $Zn_4(OH)_2(CO_3)_3{\cdot}4H_2O$ in run #3 (Table 2) show that $Mn_xZn_{(1-x)}CO_3$ solid-solutions should continue to precipitate for reaction times exceeding 24 h and the solution should finally be undersaturated with respect to $Zn_4(OH)_2(CO_3)_3{\cdot}4H_2O$. Initial supersaturation with respect to $Zn_4(OH)_2(CO_3)_3{\cdot}4H_2O$ was also observed for run #2 where the metastable formation and subsequent re-dissolution of the hydrated zinc hydroxycarbonate had probably occurred. Therefore, the suggestion is made that $Zn_4(OH)_2(CO_3)_3{\cdot}4H_2O$, which is observed in the final run #3 precipitate, is metastable under the experimental conditions used here, but that it should transform to anhydrous $Mn_xZn_{(1-x)}CO_3$ solid-solutions.

Although, to the author's knowledge, the occurrence of $Zn_4(OH)_2(CO_3)_3{\cdot}4H_2O$ has not been hitherto described from natural environments, the low-temperature formation of rhodochrosite–smithsonite solid-solutions is in accordance with the observations from the oxidized zone of the Broken Hill ore body (Birch, 1986; Böttcher *et al.*, 1993). The results of the present study indicate a complex precipitation sequence from highly supersaturated solutions, depending on the initial Zn^{2+}/Mn^{2+} ratio. However, precipitation reactions in the natural supergene environment should occur under less extreme conditions with respect to saturation indices, and the formation of some of the experimentally observed metastable phases may probably not occur. If the possible oxidation of Mn^{2+} is neglected, the final natural carbonate assemblage can be considered to mainly be a function of the CO_2 partial pressure maintained during the equilibration reactions and the dissolved transition-metal concentrations.

Acknowledgements

The author wishes to thank Prof.Dr.H.-E. Usdowski for encouraging his interest in the formation of transition-metal carbonates and Dr P.-L. Gehlken for carrying out the infrared spectroscopic measurements. The author is indebted to Drs W.D. Birch and P. Kaushansky for critically reading the manuscript, and to W.D. Birch for improving the English. Helpful suggestions on the manuscript were provided by two anonymous reviewers.

References

Ball, J.W., Nordstrom, D.K. and Zachmann, D.W. (1987) WATEQ-4F - A personal computer Fortran translation of the geochemical model WATEQ2 with revised data base. *U.S. Geol. Surv. Open-File Rep.* **87–50**.

Birch, W.D. (1986) Zinc-manganese carbonates from Broken Hill, New South Wales. *Mineral. Mag.*, **50**, 49–53.

Böttcher, M.E. (1993) *Experimental investigations of metal-enrichment reactions from aqueous solutions with relevance to ore deposits, with special regard to the formation of rhodochrosite ($MnCO_3$)* (in German). Dr.rer.nat. thesis, Georg-August-University, Göttingen.

Böttcher, M.E. and Usdowski, E. (1990) An estimation of dissociation constants for Mn(II) complexes in aqueous solutions up to 300°C. *Z. Phys. Chem. N.F.*, **167**, 81–6.

Böttcher, M.E., Gehlken, P.-L., Birch, W.D., Usdowski, E. and Hoefs, J. (1993) The rhodochrosite–smithsonite solid-solution series from Broken Hill (NSW), Australia: Geochemical and infrared spectrosopic investigations. *Neues Jahrb. Mineral., Mh.*, 352–62.

Böttcher, M.E., Gehlken, P.-L., and Usdowski, E. (1992) Infrared spectroscopic investigations of the calcite-rhodochrosite and parts of the calcite-magnesite mineral series. *Contrib. Mineral. Petrol.*, **109**, 304–6.

Effenberger, H., Mereiter, K. and Zemann, J. (1981) Crystal structure refinements of magnesite, calcite, rhodochrosite, siderite, smithsonite and dolomite, with discussion of some aspects of the stereochemistry of calcite-type carbonates. *Z. Kristall.*, **156**, 233–43.

Feitknecht, W. and Oswald, H.R. (1966) Über die Hydoxidcarbonate des Zinks. *Helv. Chim. Acta*, **49**, 335–43.

Glynn, P.D. and Reardon, E.J. (1990) Solid-solution aqueous-solution equilibria: Thermodynamic theory and representation. *Amer. J. Sci.*, **290**, 164–201.

Jambor, J.L. (1964) Studies of basic copper and zinc carbonates: I. Synthetic zinc carbonates and their relationship to hydrozincite. *Can. Mineral.*, **8**, 92–108.

Johnson, J.W., Oelkers, E.H. and Helgeson, H.C. (1992) SUPCRT92: A software package for calculating the standard molal thermodynamic properties of minerals, gases, aqueous species, and reactions from 1 to 5000 bars and 0° to 1000°C. *Comp. Geosci.*, **18**, 899–947.

Kaushansky, P. and Yariv, S. (1986) The interactions

between calcite particles and aqueous solutions of magnesium, barium and zinc chlorides. *Appl. Geochem.*, **1**, 607–18.

Kharaka, Y.K., Gunter, W.D., Aggarwal, P.K., Perkins, B.H. and DeBraal, J.D. (1988) SOLMINEQ.88: A computer program for geochemical modelling of water–rock interactions. *U.S. Geol. Surv. Wat.-Res. Inv. Rep.*, **88–4227**.

Königsberger, E., Hausner, R. and Gamsjäger, H. (1991) Solid-solute phase equilibria in aqueous solutions. V. The system $CdCO_3$–$CaCO_3$–CO_2–H_2O. *Geochim. Cosmochim. Acta*, **55**, 3505–14.

Kraut, K. (1897) Kohlensaures Zinkoxyd. *Z. anorg. Chem.*, **13**, 1–15.

La Iglesia, A. and Félix, J.F. (1994) Estimation of thermodynamic properties of mineral carbonates at high and low temperatures from the sum of the polyhedral contributions. *Geochim. Cosmochim. Acta*, **58**, 3983–91.

Lesht, D. and Bauman, J.E. (1978) Thermodynamics of the manganese(II) bicarbonate system. *Inorg. Chem.*, **17**, 3332–4.

Lorens, R.B. (1981) Sr, Cd, Mn and Co distribution coefficients in calcite as a function of precipitation rate. *Geochim. Cosmochim. Acta*, **45**, 553–61.

Mann, A.W. and Deutscher, R.L. (1980) Solution geochemistry of lead and zinc in water containing carbonate, sulphate and chloride ions. *Chem. Geol.*, **29**, 293–311.

Plummer, L.N. and Busenberg, E. (1982) The solubilities of calcite, aragonite and vaterite in CO_2–H_2O solutions between 0° and 90°C, and an evaluation of the aqueous model for the system $CaCO_3$–CO_2–H_2O. *Geochim. Cosmochim. Acta*, **46**, 1011–40.

Ryan, M.R.. and Bauman, J.E. (1978) Thermodynamics of the zinc bicarbonate system. *Inorg. Chem.*, **17**, 3329–32.

Schindler, P.W. (1967) Heterogeneous equilibria involving oxides, hydroxides, carbonates, and hydroxide carbonates. In *Equilibrium Concepts in Natural Water Systems* W. Stumm (ed.), *Adv. Chem. Ser., ACS*, **67**, 196–221.

Schindler, P., Reinert, M. and Gamsjäger, H. (1969) Zur Thermodynamik der Metallcarbonate. 3. Löslichkeitskonstanten und Freie Bildungsenthalpien von $ZnCO_3$ und $Zn_5(OH)_6(CO_3)_2$ bei 25°C. *Helv. Chim. Acta*, **52**, 2327–32.

Wagman, D.D., Evans, W.H., Parker, V.B., Schumm, R.H., Harlow, I., Bailey, S.M., Churney, K.L. and Nuttall, R.L. (1982) The NBS tables of chemical thermodynamic properties. Selected values for inorganic and C_1 and C_2 organic substances in SI units. *J. Phys. Chem. Ref. Data*, **11** Suppl. 2.

Wiwchar, B.W., Perkins, B.H. and Gunter, W.D. (1988) *Solmineq.88 PC/Shell, user manual* (Alberta Res. Counc. (ed.)).

Zachara, J.M., Kittrick, J.A., Dake, L.S. and Harshi, J.B. (1989) Solubility and surface spectroscopy of zinc precipitates on calcite. *Geochim. Cosmochim. Acta*, **53**, 9–19.

[*Manuscript received 4 August 1994: revised 12 January 1995*]